scientific reports

Check for updates

OPEN

Extracorporeal shock waves effectively suppress colorectal cancer proliferation and growth

Xiaoli Zhang[1,2]✉, Chun Ran[3]✉, Qingzhi Song[2] & Guoqing Lv[2]

Shock waves are widely used to treat various diseases and have numerous medical applications. In particular, extracorporeal shock waves (ESV) can substantially inhibit tumour growth. However, the therapeutic efficacy of ESV in colorectal cancer and its underlying mechanisms are not well understood. To address this gap in our knowledge, colorectal cancer cell lines HT29 and SW620 were used to generate xenograft mouse models and examined the therapeutic effects of a stepwise increase in ESV energy on tumour growth. In vivo, 60 mJ ESV significantly delayed xenograft growth compared with 120 and 240 mJ ESV, with no impact on body weight or hepatic and renal function. Transcriptome analysis revealed that 60 mJ ESV suppressed colorectal cancer cell proliferation and induced apoptosis and ferroptosis; these findings were further confirmed by immunohistochemical staining and western blotting. The in vitro study showed that ESV mechanistically suppressed cell proliferation and induced apoptosis and ferroptosis by activating the p53 signaling pathway. In conclusion, 60 mJ ESV substantially inhibited colorectal cancer growth by activating p53 pathway-related proliferation inhibition and cell death. These findings indicate that ESV therapy is a promising therapeutic strategy for colorectal cancer.

Keywords Extracorporeal shock waves, Colorectal cancer, P53 signaling pathway, Xenograft mouse model, Ferroptosis

Colorectal cancer (CRC) is a prevalent malignancy of the digestive tract. Moreover, it has the third-highest morbidity and second-highest mortality rates globally[1]. Surgery is the most effective treatment for CRC, particularly during the early stages of tumour development[2]. However, a substantial number of patients are diagnosed with advanced-stage disease, frequently after metastasis to distant sites in the body or when the disease is otherwise unresectable[3]. Chemotherapy and ionising radiation are occasionally used to treat high-risk CRC[4]. However, these therapeutic regimens tend to have limited efficacy because of their severe side effects and toxicity[5]. Moreover, chemotherapeutic drugs tend to kill both cancer and normal cells indiscriminately. Despite considerable advances in diagnosis and treatment, the mortality rate of patients with CRC remains high and poses a major health burden worldwide[6]. Safe and relatively effective therapeutic options for CRC must be explored to improve patient survival and prognosis.

Shock waves are supersonic pressure waves generated by shock tubes or lasers. Shock waves can deliver a sequence of transient pressure disturbances characterized by high amplitude, rapid pressure increase, short pulse duration, and rapid propagation[7]. The shock wave technique is a non-invasive, targeted, and extracorporeal therapeutic strategy with numerous medical applications[8]. Shock wave therapy has been established as a tolerable and effective method for the disintegration of urinary calculi and treatment of chronic tendinitis, bone and wound healing, and ischemic heart disease, eliciting promising results[7,9,10]. Furthermore, shock waves can increase cell membrane permeability and have been successfully used for drug delivery and gene transfer[11]. However, the application of shock-wave therapy in oncology remains poorly explored. In pre-clinical models, shock waves, especially in combination with several antineoplastic drugs, exert substantial effects. Specifically, shock waves enhance the antineoplastic effect of molecular iodine supplements in breast cancer[12]and effectively suppress the proliferation and growth of tongue squamous cell carcinoma when combined with 5-fluorouracil (5-FU)[13]. Approximately 30 years ago, shock waves were first reported to increase the chemocytotoxicity of 5-FU in CRC cells via cavitation[14]. However, research on the effects of shock waves in CRC has been limited to in vitro

[1]Department of Injury and Repair, Beijing Neurosurgical Institute, Capital Medical University, 119 Xincun Road, Fengtai District, Beijing 100000, China. [2]Department of Gastrointestinal Surgery, Peking University Shenzhen Hospital, Guangdong 518000, China. [3]China Ordnance Society, 10 Chedaogou, Haidian District, Beijing 100000, China. ✉email: nanyuxiaoxiao@163.com; rangle123@163.com

cytotoxicity and lacks comprehensive investigations into the underlying mechanisms. Moreover, the therapeutic effects of shock waves alone on CRC are unknown.

p53, also known as the guardian of the genome, is a classic tumour suppressor that limits cellular proliferation by inducing cell cycle arrest, apoptosis and ferroptosis[15–17]. *p53* is activated by various stress signals, including DNA damage and oncogene activation and it orchestrates a plethora of downstream responses, such as DNA repair, cell cycle arrest, senescence, metabolism, and cell death[17,18]. Several chemotherapy regimens and radiotherapy rely on *p53* activation and its downstream responses to impede cancer cell growth. The activation of *p53* for induction of p53-related outcomes, such as cell death, in response to cancer therapy has been explored to improve clinical outcomes[19,20]. Therefore, identifying therapies capable of targeting *p53* may represent a promising therapeutic strategy for CRC. We hypothesised that shock waves could activate *p53*-related cancer inhibition. To investigate this, we assessed the therapeutic effect of ESV alone in CRC xenograft mouse models. Furthermore, we explored the potential molecular mechanisms of ESV-mediated inhibition of CRC growth.

Results

Effects of stepwise increases in ESV energy on CRC xenograft tumour growth

To determine the therapeutic effect of ESV in vivo, a mouse model of subcutaneous tumours was established. Nude mice were subcutaneously injected with HT29 cells and tumour growth was observed daily (Fig. 1A). When the average tumour volume was approximately 50 mm^3, ESV therapy (60, 120, and 240 mJ for 2000 shots) was administered every third day (Fig. 1B; supplementary Fig. 1). Body weight and tumour volume were measured at different time points (days 0, 3, 6, and 9 after ESV therapy). No significant changes were observed in body weight (Fig. 1C). Compared with day 0, Tumours increased in size by 262.8% in the control group

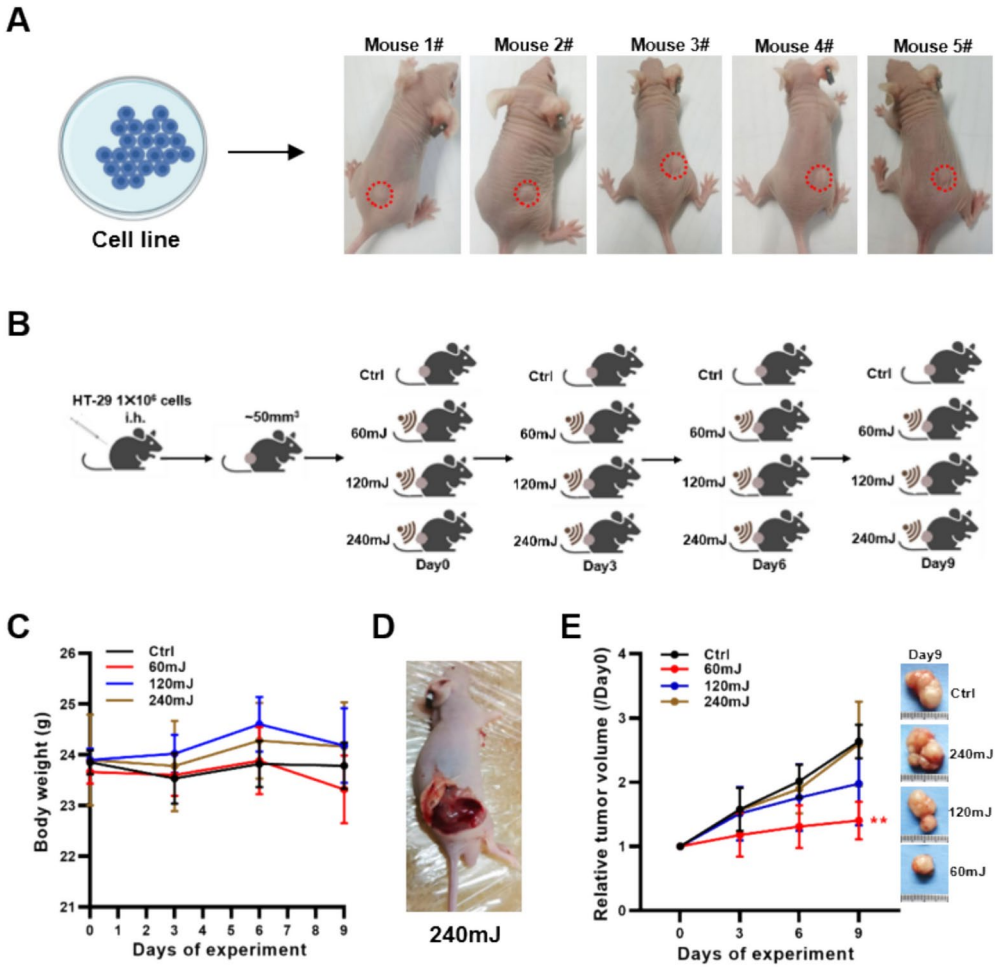

Fig. 1. Impact of stepwise increased dosage of ESV energy on CRC xenograft tumour growth. **A** Establishment of HT29-derived transplant tumour model in nude mice. **B** Schematic representation of increased dosages of ESV energy (60 mJ, 120 mJ and 240 mJ, 2000 shots, 12 Hz) at different time (every third day) in CRC xenograft model. **C** Body weights of control (Ctrl), 60 mJ, 120 mJ, and 240 mJ mice (n = 5). **D** The anatomy view of a mouse in 240 mJ group. **E** Relative tumour volumes at day 0, day 3, day 6, day 9 after the first ESV treatment (n = 5), and the representative images of tumours at the end of experiment. Tumour volume = (width^2 × length)/2. Statistical significance was determined using one-way ANOVA with Tukey's test. $^{**}p < 0.01$.

on day 9. Administration of 60 mJ ESV significantly suppressed tumour growth, resulting in growth of only 141% ($p < 0.01$). The administration of 120 mJ ESV generated weak and non-significant inhibition, eliciting tumour growth of 197%, whereas 240 mJ ESV exerted no suppressive effect on tumour growth (249.3%, Fig. 1E). Examination of the animals after their final treatment show that those in the 240 mJ ESV group exhibited bruises, suggesting significant vascular lesions (Fig. 1D). After screening for ESV energy in the CRC xenograft mouse model, 60 mJ ESV was selected for subsequent in vivo experiments.

Administration of 60 mJ ESV delays the growth of CRC-derived xenografts

To validate the therapeutic impact of 60 mJ ESV on CRC, we extended the experimental endpoint (days 0, 3, 6, 9, 12, and 15 after ESV therapy) and examined the side effects. In the second set of experiments, the weight of the mice was unaltered, consistent with the results of the previous experiment (Fig. 2A). Plasma alanine aminotransferase (ALT) and creatinine (Cr) levels are biomarkers of hepatic and renal function, respectively. No differences were observed in serum ALT and Cr levels between the control and 60 mJ ESV groups, indicating that 60 mJ ESV did not induce notable toxicity (Fig. 2B, C). Mice administered ESV had slower tumour growth than mice in the control group (Fig. 2D). At the experimental endpoint (day 15), mice in the 60 mJ ESV group had smaller tumours than mice in the control group (Fig. 2E). Pathological examination revealed the absence of notable liver abnormalities, indicating no liver metastasis (Fig. 2F). In addition, the administration of 60 mJ ESV suppressed the growth of SW620-derived xenografts, another colorectal cancer cell line (supplementary Fig. 2). These results suggest that 60 mJ ESV can effectively suppress CRC growth in vivo without inducing toxicity.

Administration of 60 mJ ESV blocks CRC cell proliferation

To elucidate the mechanisms through which shock waves inhibit CRC growth in transplant models, transcriptome analysis was performed using HT29-derived tumour tissues from the control (CON) and 60 mJ groups. RNA-Seq captures the transcriptional information of cells in a fixed state and provides a snapshot of the DNA expression profile at specific time points. RNA-Seq revealed that 60 mJ ESV reprogrammed the transcriptome, with 1748 upregulated genes and 2021 downregulated genes (Fig. 3A, B). Metascape was used to analyse differentially expressed genes between the two groups. Downregulated differentially expressed genes were primarily enriched in the 'DNA metabolic process' and 'mitotic cell cycle' (Fig. 3C). Mitosis is the basis for cell proliferation. Typically, tumour cells have abnormally active mitotic abilities and can rapidly proliferate. According to the RNA-seq data, the administration of 60 mJ ESV suppressed the proliferation of CRC cells. Ki-67 staining was performed to evaluate cell proliferation. The tumour tissues in the 60 mJ ESV group showed lower Ki-67 staining compared with those in control group (Fig. 3D; supplementary Fig. 4). These results indicate that ESV may exert therapeutic effects by suppressing the proliferation of CRC cells.

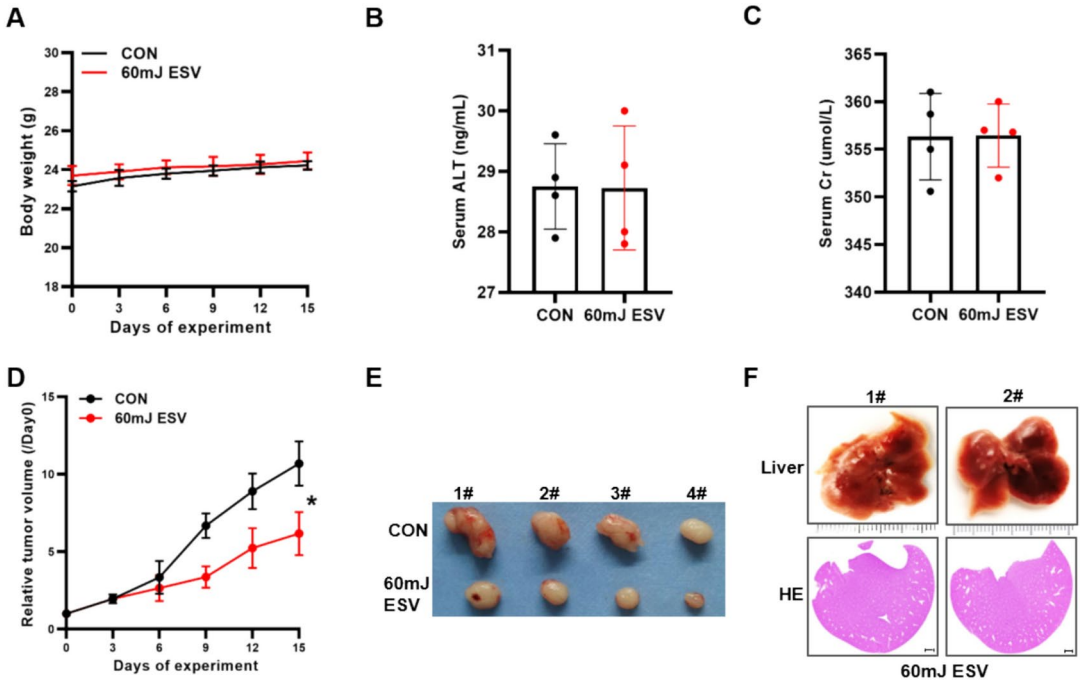

Fig. 2. 60 mJ ESV suppresses the growth of HT29-derived xenografts. **A** Body weights of control (CON) and 60 mJ mice (n = 4). **B–C** Serum alanine aminotransferase (ALT) and creatinine (Cr) in plasma (n = 4). **D** Relative tumour volumes at day 0, day 3, day 6, day 9, day 12 and day 15 after the first ESV treatment (n = 4). **E** Images of tumours at the end of the experiment (n = 4). **F** Mouse livers of 60 mJ ESV group at the end of the experiment (n = 2). Representative pictures of H&E staining of paraffin-embedded liver sections (Scale: 100 μm). Data are presented as means ± SD of three independent experiments. Statistical significance was determined using one-way ANOVA with Tukey's test. *$p < 0.05$.

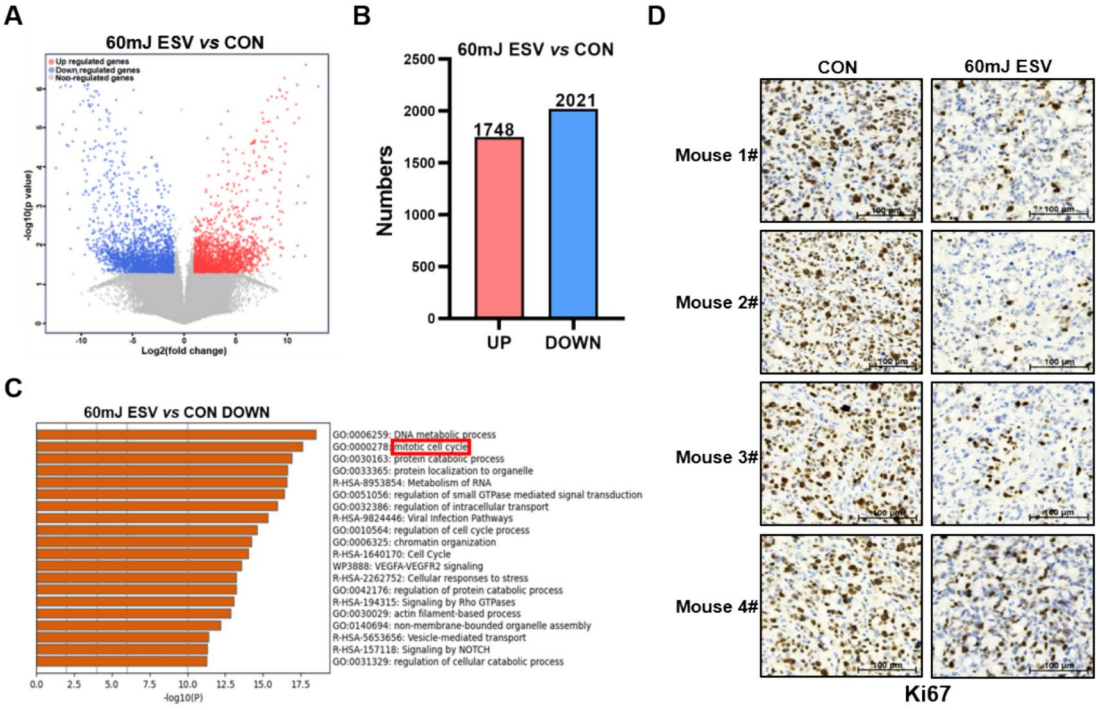

Fig. 3. 60 mJ ESV blocks the proliferation of CRC cells. **A** Volcano plot representing transcriptome differences between CON and 60 mJ ESV group. **B** The number of differentially expressed genes between CON and 60 mJ ESV group. **C** Metascape analysis of downregulated genes in 60 mJ ESV group. **D** Ki67-staining (Scale: 100 μm).

ESV induces apoptosis and ferroptosis in CRC cells

Cell death and cell cycle arrest contribute to the inhibition of cell proliferation. To explore the mechanism through which ESV blocks CRC cell growth, we performed a gene set enrichment analysis (GSEA). Genes upregulated in the ESV group were enriched in pathways associated with apoptosis (Fig. 4A). Based on western blot analysis, the application of ESV increased the expression of the apoptosis biomarkers cleaved-PARP and cleaved-caspase3 (Fig. 4B, C). IHC staining also verified the upregulated expression of cleaved-caspase3 in the ESV group (Fig. 4D; supplementary Fig. 4A). Moreover, the ferroptosis biomarkers AKR1C1 and COX2 were increased in the ESV group compared with the control group (Fig. 4E–G; supplementary Fig. 4B). These findings indicate that ESV can substantially induce apoptosis and ferroptosis in CRC tissues.

ESV effects on cell proliferation and death are related to the p53 pathway

To determine the potential pathway involved in ESV-mediated CRC inhibition, Metascape and GSEA analyses were applied to the RNA-seq data. The results revealed the enrichment of the *p53* signaling pathway gene set in the ESV group (Fig. 5A, B). Given that the *p53* signaling pathway is a classic tumour suppressor that plays an important role in tumour regulation, we speculated that ESV could inhibit CRC growth via this pathway. We detected *p53* mRNA and protein levels in HT29-derived tumours using real-time PCR and western blotting, respectively. ESV-treated mice exhibited upregulated p53 expression compared with control mice; this enhanced expression was confirmed by IHC staining for p53 (Fig. 5C–F; supplementary Fig. 4C). Collectively, these results suggest that ESV can suppress cell proliferation and induce apoptosis and ferroptosis by upregulating p53 expression in vivo.

ESV inhibits proliferation and promotes the death of CRC cells in vitro

In addition to the above in vivo animal experiments, we performed in vitro cell experiments. The CCK-8 assay showed that 60 mJ ESV markedly suppressed the proliferation of HT29 and SW620 cells in vitro (Fig. 6A; supplementary Fig. 5A). Flow cytometric analysis revealed that ESV-treated CRC cells had more cells in the G0/G1 phase (77.3%) than control cells (60.6%). ESV-treated cells were arrested at the G0/G1 phase of the cell cycle and the percentage of cells in the S phase was reduced (Fig. 6B; supplementary Fig. 5B). Furthermore, flow cytometric analysis showed that treatment with ESV significantly increased the percentage of dead HT29 cells (PI^+ cells, Fig. 6C; supplementary Fig. 5C). Treatment with ESV increased the levels of P53 protein in vitro, along with those of cleaved-PARP, cleaved-caspase3, AKR1C1, and COX2 (Fig. 6D, E). Collectively, these findings indicate that ESV could impede CRC growth via p53 pathway-mediated cell cycle arrest and cell death, both in vivo and in vitro.

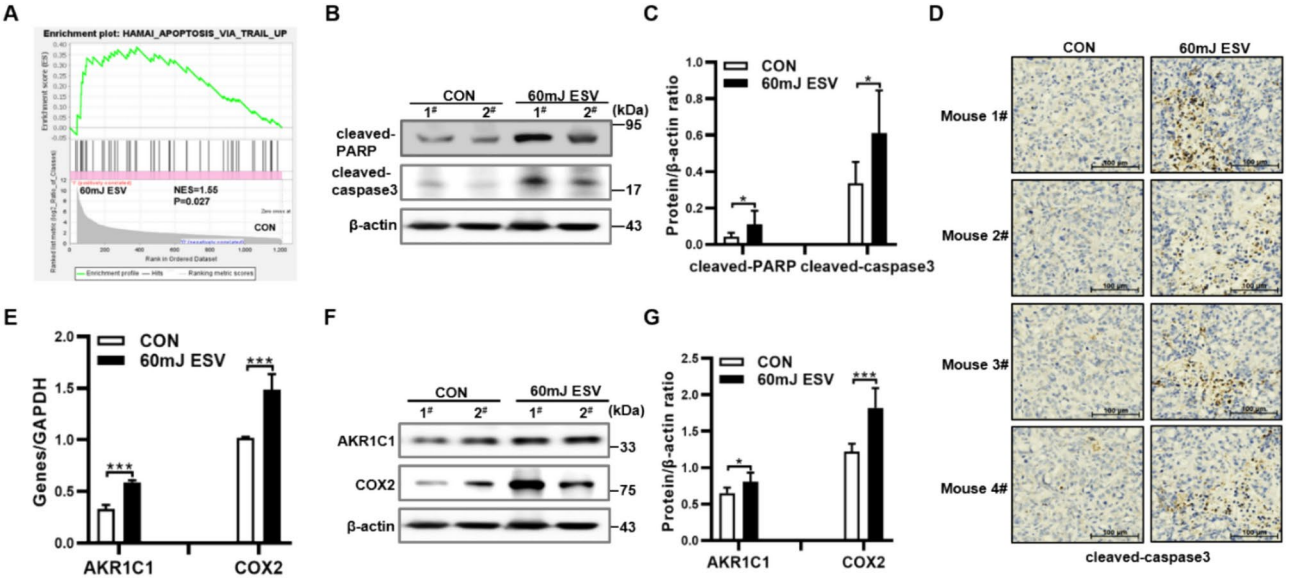

Fig. 4. 60 mJ ESV induces apoptosis and ferroptosis in CRC cells. **A** Gene set enrichment analysis plots for apoptosis. NES, normalized enrichment score; Black bars represent genes contained within the specific pathway ranked from positively expressed (left) to negatively expressed (right) based on log twofold change (60 mJ ESV *vs*. CON). **B** Western blot analysis of cleaved-PARP and cleaved-caspase3. **C** cleaved-PARP and cleaved-caspase3 densitometry relative to β-actin. **D** cleaved-caspase3 staining (Scale: 100 μm). **E** The relative mRNA levels of *AKR1C1* and *COX2* measured by real-time PCR. **F** Western blot analysis of AKR1C1 and COX2. **G** AKR1C1 and COX2 densitometry relative to β-actin. $^{*}p < 0.05$, $^{***}p < 0.001$.

Discussion

In this study, we investigated the effects of ESV monotherapy against CRC growth both in vivo and in vitro and notable preclinical implications were identified. Firstly, animal experiments revealed that the administration of 60 mJ ESV decreased tumour growth without affecting body weight or liver and kidney functions. Secondly, in vivo and in vitro studies revealed ESV treatment suppressed CRC cell proliferation and induced apoptosis and ferroptosis. Thirdly, ESV therapy was determined to exert tumour-suppressive effects by reactivating the p53 signaling pathway. These results indicate that ESV therapy may be an effective therapeutic modality for suppressing CRC growth.

Currently, effective and safe methods for treat patients with advanced-stage or unresectable cancer are lacking[21]. Therefore, ESV, which is non-invasive and targeted, could be a valuable cancer treatment and its inhibition of CRC was evaluated. ESV is most suitable for application to relatively superficial tissues and organs. ESV was found to effectively suppress the proliferation and growth of tongue squamous cell carcinoma and breast cancer, which are relatively superficial types of cancer in the human body[12,13]. Importantly, specific instruments to administer shock-wave therapy in patients with breast cancer have been developed and are undergoing preliminary clinical trials. The most important finding of our study was that administration of ESV alone could significantly reduce the tumour volume in nude mice with CRC transplanted subcutaneously, which is an animal model with a superficial tumour. However, colorectal tumours are located in the abdominal cavity rather than on the body surface. Further studies are required to explore the therapeutic effects of ESV using spontaneous CRC models, such as the $APC^{min/+}$mouse or azoxymethane/dextran sulfate sodium-induced mouse colitis-associated carcinogenesis model[22].

Thirty years ago, scientists explored the potential of shock waves as a tumour treatment. Shock waves can shatter tumour cells and injure the microvasculature, raising concerns regarding the risk of metastasis[23,24]. Subsequent studies revealed that the effects of shock waves on tumours depended on the shockwave energy. Aceves C et al. revealed that high-dose shock wave treatment (SW150/21.7 MPa) generated tissue lesions without decreasing tumour growth and promoted pro-tumour conditions. Conversely, low (SW35/9.9 MPa) shock wave doses had notable antineoplastic effects in breast cancer therapy[12]. Some studies have found that low-dose shock waves enhance free radical generation, ATP release, or membrane instability, which could induce apoptotic mechanisms, ultimately reducing tumour growth and diminishing the potential for tumour metastasis[25]. Consistent with these findings, our study investigated three different shock wave energies, demonstrating that low-energy (60 mJ) shock waves remarkably blocked CRC growth without liver metastasis. Conversely, 240 mJ failed to inhibit tumour growth and caused haematoma. However, lower energy ESV may not necessarily have a more significant anticancer effect. Compared with 60 mJ ESV, 30 mJ ESV did not inhibit the growth of CRC cells (supplementary Fig. 6). The shock waves may induce permanent damage to tumour cells, requiring a certain amount of energy deposition[26], and the lack of cell death may be because the stress is below the damage threshold. Therefore, the damage threshold of ESV in CRC cells should be further investigated.

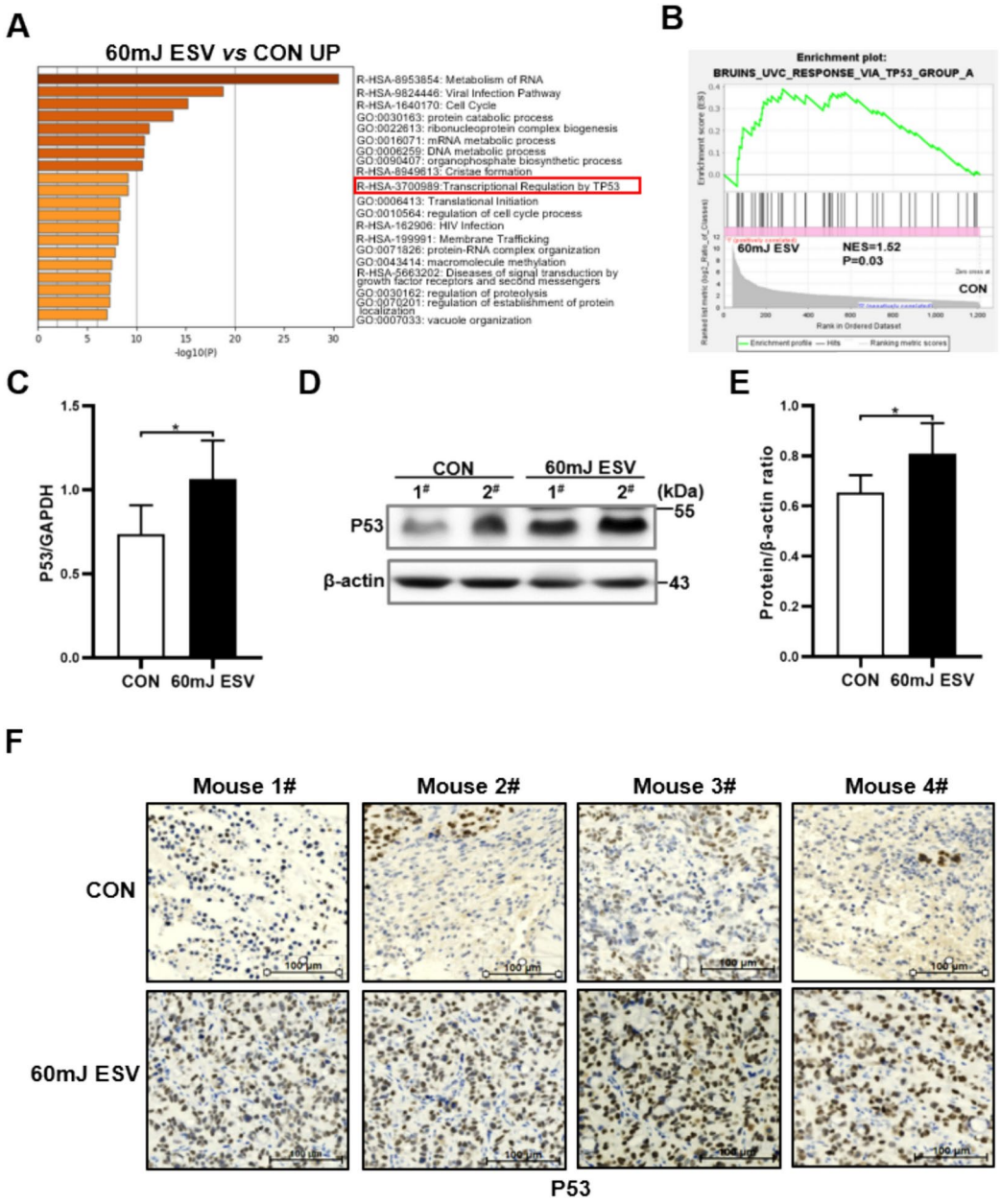

Fig. 5. Effect of 60 mJ ESV on cell proliferation and death is related to *p53* pathway. **A** Metascape analysis of upregulated genes in 60 mJ ESV group. **B** Gene set enrichment analysis plots for *p53* pathway. **C** The relative mRNA level of *p53* measured by real-time PCR. **D** Western blot analysis of P53. **E** P53 densitometry relative to β-actin. **F** P53 staining (Scale: 100 μm). Statistical significance was determined using one-way ANOVA with Tukey's test. $^*p < 0.05$.

In addition to energy, other mechanical parameters of shock waves, including peak pressure, rise time, and shock wave impulse, can also impact therapeutic outcomes. Schmidt et al.conducted in vitro experiments to examine the effects of shock waves on U87 brain cancer cells. The authors found that when the incident peak pressure exceeded a lethal level, shock waves could induce substantial cell damage[27]. Liao et al.found that shock waves with higher impulses decreased cell viability, whereas shock waves with similar peak pressures exerted distinct effects on cell viability[28]. In this study, we focused on the effects of shock waves of different energies on CRC growth. Additional studies are required to investigate the effects of other mechanical characteristics of shock waves on CRC cell viability.

In conclusion, we present new in vivo and in vitro evidences demonstrating a novel method for treating CRC. The use of 60 mJ ESV could markedly suppress CRC growth by blocking the proliferation of cancer cells and inducing apoptosis and ferroptosis. Mechanistically, ESV may activate the p53 signaling pathway to inhibit CRC growth. Our study highlights that appropriate ESV energy may serve as an accessory option (i.e., 'give it a try') for patients with terminal-stage CRC who are refractory to conventional therapy.

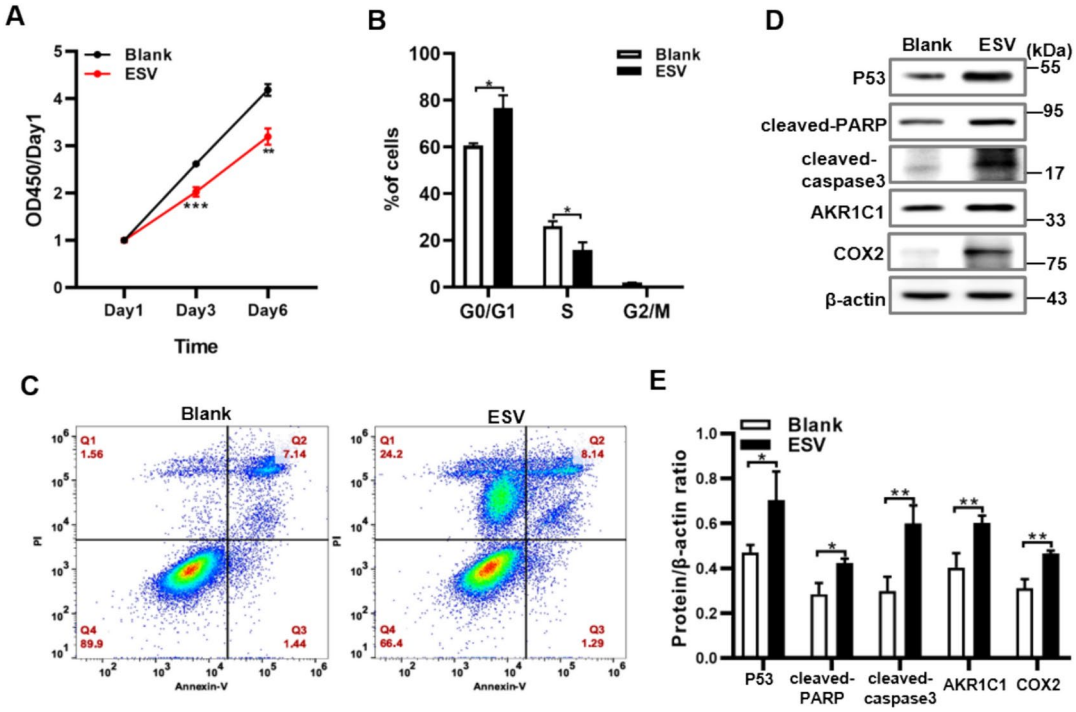

Fig. 6.. 60 mJ ESV inhibits proliferation and promotes death of CRC cells in vitro. **A** HT29 cell viability at day 3 and day 6 after treatment with 60 mJ ESV, 2000 shots, 12 Hz. **B** Cells were analyzed by flow cytometry to determine the percentage of cells in the indicated cell cycle phases. **C** Cells were analyzed by flow cytometry to determine the percentage of death cells. **D** Western blot analysis of P53, cleaved-PARP, cleaved-caspase3, AKR1C1 and COX2. **E** P53, cleaved-PARP, cleaved-caspase3, AKR1C1 and COX2 densitometry relative to β-actin. Data are presented as means ± SD of three independent experiments. Statistical significance was determined using one-way ANOVA with Tukey's test. $^{*}p < 0.05$, $^{**}p < 0.01$, $^{***}p < 0.001$.

Materials and methods

Mouse xenograft studies

All protocols for animal procedures were approved by the ethics committee of Beijing Neurosurgical Institute Ethics Committee of Capital Medical University (BNI202304002). Six-to-eight-week-old male BALB/c nude mice were purchased from Beijing Vital River Laboratory Animal Technology Co. Ltd. (Beijing, China) and subcutaneously injected with 1×10^6 HT29 or SW620 in 100 μL. The mice were observed daily for tumour growth. When the average tumour volume reached approximately 50 mm^3, the mice were divided randomly into four groups, including control (Ctrl), 60 mJ, 120 mJ, and 240 mJ shock waves groups. The control group without any treatment, shock waves groups accepted ESV therapy with stepwise increased energy (60, 120, 240 mJ, 2000 shots, 12 Hz) at days 0, 3, 6, 9 and 12 after therapy initiation. At the same time, the tumour volumes were measured once every 3 days to determine the effect of each therapeutic regimen. The lengths (L) and widths (W) of the tumours were measured, and the tumour volumes were calculated as $(L \times W^2)/2$. All experiments were performed according to the relevant guidelines, regulations, and ARRIVE guidelines.

ESV application and definition

The ESV machine, called lattice shock wave physiotherapy instrument (J Gendica, China), was utilized in the present study. In detail, the ESV energy could be adjusted prior to applying for the in vitro and in vivo studies. After a determination of machine parameters, the machine was switched on. The automatic shots to the specific tissues/cells were started on. We defined the ESV energy applied to animals as 60 mJ, 120 mJ, and 240 mJ (2000 shots, 12 Hz). Additionally, we defined the ESV energy applied to HT29 and SW620 cell lines as 60 mJ, 2000 shots, 12 Hz.

RNA sequencing

RNA samples were prepared from three biological replicates of HT29-derived xenograft tissues using TRIzol reagent. RNA quality was quantified using RNA integrity number. Sequencing libraries were constructed using the NEB Next Ultra RNA Library Prep Kit for Illumina and quantified using the KAPA Library Quantification kit (KAPA Biosystems). The libraries were then sequenced on an Illumina HiSeq sequencer. 150 bp paired-end reads were mapped to human hg19 genome. Cuffdiff was used to analyze differentially expressed genes between the samples.

Immunohistochemistry (IHC) analysis

Paraffin-embedded xenografts were cut into 4 mm sections. The sections were dewaxed and hydrated, and then blocked and incubated with primary antibodies against Ki67 (Cell Signaling Technology, 12202, 1:200), P53 (Proteintech, 60283-2-Ig, 1:1000), cleaved-caspase3 (Cell Signaling Technology, 9664T, 1:1000) at 4 °C overnight. The signals were visualized using a two-step plus®Poly-HRP Anti-Mouse/Rabbit IgG Detection System (OriGene, PV9000). Counterstaining was performed using hematoxylin. The sections were digitally scanned under a microscope with an FL-20 cooled camera, and images were analyzed using the Mosaic™ V2.1 software.

Reverse transcription-quantitative polymerase chain reaction

The total RNA content was isolated from cells or the tumour using TRIzol™ reagent (Invitrogen), treated with DNase I (Thermo Fisher Scientific, Cat# EN0521), and then reverse transcribed into cDNA using a Maximal First Strand cDNA Synthesis Kit (Thermo Fisher Scientific, Cat# K1622). Real-time polymerase chain reaction (PCR) was performed using an S1000 PCR instrument (Bio-Rad, Hercules, CA, USA) to quantify gene expression. The PCR data were normalized to glyceraldehyde-3-phosphate dehydrogenase expression at the mRNA level. The primers used are listed in Supplementary Table S1.

Western blotting

Proteins were extracted from tumour tissues or cells with RIPA buffer (0.01% EDTA, 0.1% TritonX-100 and 10% proteinase inhibitor cocktail). Protein concentrations were quantified with a protein assay kit (Bio-Rad). 100 μg lysate were separated on 10% SDS-PAGE gel and transferred to polyvinylidene difluoride membranes. The membranes were probed overnight at 4 °C with primary antibody against human P53 (Cell Signaling Technology, 48818S, 1:1000), β-actin (Sigma, 1:10,000), cleaved-caspase3 (Cell Signaling Technology, 9664T, 1:1000), cleaved-PARP (Cell Signaling Technology, 9541T, 1:1000), AKR1C1 (Abcam, ab192785, 1:1000), COX2 (Abcam, ab179800, 1:1000), followed by incubation with peroxidase-conjugated secondary antibody (Cell Signaling Technology, 1:10,000) for 1.5 h. The signal was visualized with ECL (Millipore).

Statistical analysis

All experiments were independently repeated at least three times unless stated otherwise. Statistical analyses were performed using the GraphPad Prism software (version 8.0). Data are presented as the mean ± standard deviation (SD). Two groups were compared using the Student's t-test for unpaired data. Comparisons among more than two groups were performed using ANOVA and Tukey's test. For all tests, P values ≤ 0.05, were considered statistically significant ($^*P < 0.05$).

Data availability

The datasets generated and analysed during the current study are available in the Gene Expression Omnibus (https://www.ncbi.nlm.nih.gov/geo/) with GSE290314.

Received: 22 August 2024; Accepted: 13 March 2025
Published online: 21 March 2025

References

1. Sung, H. et al. Global cancer statistics 2020: GLOBOCAN estimates of incidence and mortality worldwide for 36 cancers in 185 countries. *CA Cancer J. Clin.* **71**, 209–249. https://doi.org/10.3322/caac.21660 (2021).
2. Zhang, X. et al. Glutathione peroxidase 4 as a therapeutic target for anti-colorectal cancer drug-tolerant persister cells. *Front. Oncol.* https://doi.org/10.3389/fonc.2022.913669 (2022).
3. Cañellas-Socias, A. et al. Metastatic recurrence in colorectal cancer arises from residual EMP1(+) cells. *Nature* **611**, 603–613. https://doi.org/10.1038/s41586-022-05402-9 (2022).
4. Dariya, B., Aliya, S., Merchant, N., Alam, A. & Nagaraju, G. P. Colorectal cancer biology, diagnosis, and therapeutic approaches. *Crit. Rev. Oncog.* **25**, 71–94. https://doi.org/10.1615/CritRevOncog.2020035067 (2020).
5. Rehman, S. K. et al. Colorectal cancer cells enter a diapause-like DTP state to survive chemotherapy. *Cell* **184**, 226-242.e221. https://doi.org/10.1016/j.cell.2020.11.018 (2021).
6. Ionescu, V. A., Gheorghe, G., Bacalbasa, N., Chiotoroiu, A. L. & Diaconu, C. Colorectal cancer: from risk factors to oncogenesis. *Medicina (Kaunas)* **59**, 1646. https://doi.org/10.3390/medicina59091646 (2023).
7. Nishida, T. et al. Extracorporeal cardiac shock wave therapy markedly ameliorates ischemia-induced myocardial dysfunction in pigs in vivo. *Circulation* **110**, 3055–3061. https://doi.org/10.1161/01.Cir.0000148849.51177.97 (2004).
8. Chen, H. et al. Recent progress in development of new sonosensitizers for sonodynamic cancer therapy. *Drug Discov. Today* **19**, 502–509. https://doi.org/10.1016/j.drudis.2014.01.010 (2014).
9. Rompe, J. D., Zoellner, J. & Nafe, B. Shock wave therapy versus conventional surgery in the treatment of calcifying tendinitis of the shoulder. *Clin. Orthop. Relat. Res.* **387**, 72–82. https://doi.org/10.1097/00003086-200106000-00010 (2001).
10. Wang, L. et al. Extracorporeal shock wave therapy in treatment of delayed bone-tendon healing. *Am. J. Sports Med.* **36**, 340–347. https://doi.org/10.1177/0363546507307402 (2008).
11. Kodama, T., Doukas, A. G. & Hamblin, M. R. Shock wave-mediated molecular delivery into cells. *Biochim. Biophys. Acta* **1542**, 186–194. https://doi.org/10.1016/s0167-4889(01)00177-x (2002).
12. Peña, M. et al. Shock wave application increases the antineoplastic effect of molecular Iodine supplement in breast cancer xenografts. *Ultrasound Med. Biol.* **46**, 649–659. https://doi.org/10.1016/j.ultrasmedbio.2019.11.015 (2020).
13. Chang, C. L. et al. Combined high energy of extracorporeal shock wave and 5-FU effectively suppressed the proliferation and growth of tongue squamous cell carcinoma. *Biomed. Pharmacother.* **142**, 112036. https://doi.org/10.1016/j.biopha.2021.112036 (2021).
14. Prat, F. et al. Increased chemocytotoxicity to colon cancer cells by shock wave-induced cavitation. *Gastroenterology* **106**, 937–944. https://doi.org/10.1016/0016-5085(94)90752-8 (1994).
15. Symonds, H. et al. p53-dependent apoptosis suppresses tumor growth and progression in vivo. *Cell* **78**, 703–711. https://doi.org/10.1016/0092-8674(94)90534-7 (1994).

16. Liu, F. et al. Downregulation of CPT2 promotes proliferation and inhibits apoptosis through p53 pathway in colorectal cancer. *Cell Signal* **92**, 110267. https://doi.org/10.1016/j.cellsig.2022.110267 (2022).
17. Jiang, L. et al. Ferroptosis as a p53-mediated activity during tumour suppression. *Nature* **520**, 57–62 (2015).
18. Oren, M. & Prives, C. p53: A tale of complexity and context. *Cell* **187**, 1569–1573. https://doi.org/10.1016/j.cell.2024.02.043 (2024).
19. Hassin, O. & Oren, M. Drugging p53 in cancer: one protein, many targets. *Nat. Rev. Drug Discov.* **22**, 127–144. https://doi.org/10.1038/s41573-022-00571-8 (2023).
20. Peuget, S., Zhou, X. & Selivanova, G. Translating p53-based therapies for cancer into the clinic. *Nat. Rev. Cancer* **24**, 192–215. https://doi.org/10.1038/s41568-023-00658-3 (2024).
21. Rawla, P., Sunkara, T. & Barsouk, A. Epidemiology of colorectal cancer: incidence, mortality, survival, and risk factors. *Prz Gastroenterol.* **14**, 89–103. https://doi.org/10.5114/pg.2018.81072 (2019).
22. Zhang, X. et al. High-fat diet aggravates colitis-associated carcinogenesis by evading ferroptosis in the ER stress-mediated pathway. *Free Radic. Biol. Med.* **177**, 156–166. https://doi.org/10.1016/j.freeradbiomed.2021.10.022 (2021).
23. Dellian, M. et al. High-energy shock waves enhance hyperthermic response of tumors: Effects on blood flow, energy metabolism, and tumor growth. *J. Natl. Cancer Inst.* **86**, 287–293. https://doi.org/10.1093/jnci/86.4.287 (1994).
24. Oosterhof, G. O., Cornel, E. B., Smits, G. A., Debruyne, F. M. & Schalken, J. A. The influence of high-energy shock waves on the development of metastases. *Ultrasound Med. Biol.* **22**, 339–344. https://doi.org/10.1016/0301-5629(95)02051-9 (1996).
25. López-Marín, L. M. et al. Shock wave-induced damage and poration in eukaryotic cell membranes. *J. Membr. Biol.* **250**, 41–52. https://doi.org/10.1007/s00232-016-9921-2 (2017).
26. Li, D. et al. Response of single cells to shock waves and numerically optimized waveforms for cancer therapy. *Biophys. J.* **114**, 1433–1439. https://doi.org/10.1016/j.bpj.2017.09.042 (2018).
27. Schmidt, M. et al. Characterization of a setup to test the impact of high-amplitude pressure waves on living cells. *Sci. Rep.* **4**, 3849. https://doi.org/10.1038/srep03849 (2014).
28. Liao, Y. et al. Shock wave impact on the viability of MDA-MB-231 cells. *PLoS One* **15**, e0234138. https://doi.org/10.1371/journal.pone.0234138 (2020).

Author contributions
XLZ and QZS performed the experiments. XLZ and CR designed experimental protocols, interpreted data obtained from the experiments, and wrote the manuscript. GQL edited the manuscript.

Funding
This work was supported by the National Nature Science Foundation of China (82203229); the Shenzhen Science and Technology Program (JCYJ20220531094005012), and the opening project of State Key Laboratory of Explosion Science and Technology (Beijing Institute of Technology, KFJJ22-16M).

Declarations

Competing interests
The authors declare no competing interests.

Ethic statement
Our studies did not include human participants, human data or human tissue. All the animal protocols containing all the procedures were approved by the ethics committee of Beijing Neurosurgical Institute Ethics Committee of Capital Medical University, and were performed in accordance with all regulatory standards.

Additional information
Supplementary Information The online version contains supplementary material available at https://doi.org/10.1038/s41598-025-94386-3.

Correspondence and requests for materials should be addressed to X.Z. or C.R.